# Operando neutron scattering: following reactions in real time using neutrons

Vainius Skukauskas, Elliot L.B. Johnson Humphrey, Iain Hitchcock, Andrew York, Joseph Kelleher, Emma K. Gibson, David J. Nelson, Ian. P. Silverwood

# *Operando* Neutron Scattering – Following Reactions in Real Time Using Neutrons

Vainius Skukauskas[1a], Elliot L.B. Johnson Humphrey[2b], Iain Hitchcock[3], Andrew York[3c], Joseph Kelleher[4], Emma K. Gibson[1d], David J. Nelson[2e], Ian. P. Silverwood[4f]

1: University of Glasgow, School of Chemistry, Glasgow, UK

2: University of Strathclyde, WestCHEM Department of Pure and Applied Chemistry, University of Strathclyde, Glasgow, UK

3: Johnson Matthey Technology Centre, Sonning Common, Oxon, UK

4: ISIS Neutron and Muon Facility, Rutherford Appleton Laboratory, Harwell Campus, Chilton, Oxon, UK

a: https://orcid.org/0000-0001-6858-4506
b: https://orcid.org/0000-0001-6615-3411
c: https://orcid.org/0000-0001-5857-7089
d: https://orcid.org/0000-0002-7839-3786
e: https://orcid.org/0000-0002-9461-5182
f: Corresponding author ian.silverwood@stfc.ac.uk https://orcid.org/0000-0002-6977-1976

Keywords: Operando; Catalysis; Neutron Diffraction; Quasielastic Neutron Scattering; QENS

## Abstract

The complexation of $NiCl_2$ with 2,2'-Bipyridine was followed using quasielastic neutron scattering to observe reaction progress. Water adsorption in chabazite with time resolution was observed using strain induced in the aluminosilicate framework with a high-resolution engineering diffractometer. These reactions illustrate the recent progress and possibilities in using neutron probes to observe realistic catalytic reactions as they progress.

## Introduction

In the field of catalysis, understanding the relationship between the catalyst structure and the selectivity/reactivity is fundamental for the rational development of future reaction processes. Catalytic systems alter with changes in environmental conditions such as temperature, pressure and gas/liquid composition; establishing these relationships between structure and performance under relevant conditions is thus vital for optimum catalyst design. [1]

*In situ* spectroscopy is indispensable for the characterisation of catalysts in a multitude of chemical reactors and environmental cells. [1,2] Despite *in situ* studies enabling catalyst observation under controlled conditions, lack of reaction product analysis prevents a direct relationship between structure (surface/bulk) and performance (activity/selectivity) from being deduced – especially when employing vacuum or non-reaction conditions. [1] Combining time-resolved *in situ* characterisation with online reaction product analysis gives rise to *operando* spectroscopy, [2,3] where both the catalyst characterisation and the product analysis are performed simultaneously.

Neutrons' ability to interact with nuclei of atoms allow penetration deep into a catalyst bed, or through thick reactor walls necessary for reactions in extreme conditions; as well as preserving the integrity of the

sample which can often be altered or damaged by other techniques such as x-rays. This weak interaction, coupled with the difficulty creating intense sources result in neutron flux limiting the technique. Larger samples are required and extended data collection times, which limits the time-resolution possible during in situ measurement. Nevertheless, neutrons have been extensively exploited for the study of functional materials: [4] using neutron diffraction to elucidate the positions of adsorbed hydrogen-containing molecules within microporous catalysts [5,6] and probing reaction kinetics. [7] Neutron diffraction techniques are well suited for operando studies, such as those reported for batteries, [8] proton conductors, [9] catalysts [10-13] and ammonia storage. [14-17]

Incoherent inelastic neutron scattering (IINS) involves a significant transfer of energy ($\Delta E \neq 0$) which corresponds to the energy required to excite vibrational quanta of the analyte. [17] This technique is mostly restricted to vibrational modes that involve H atoms, due to hydrogen's inherent, exceptionally large incoherent scattering cross section. [18] This property has been exploited in studies of catalyst deactivation and coking, [19-22] catalyst supports, [23] and reaction intermediates. [24] Furthermore, INS was used to study adsorption of ethene and propene on carbon [25] as well as the interaction of methanol with η-alumina. [26] Neutron spectroscopy is more severely impacted by flux-limitation as the inelastic scatter is much weaker than the elastic scattering at practical measurement temperatures. Another limitation in terms of in situ and operando studies, is the Debye-Waller factor of the scattering law. [17,27] This describes the thermal motion of the system and leads to extreme broadening of the peaks, resulting in a decreased resolution and 'smearing out' of features. This can be reduced by cooling the sample; ergo spectra are typically recorded below 30 K, [28] limiting its application to studies under practical operating conditions. Hence, a "react & quench" approach has been implemented in most in situ INS studies. [29,30] Nevertheless, an operando INS method was described by Parker in 2011 during a study on the role of hydroxyl groups in low temperature CO oxidation. [31] It was thus shown that it is possible to eschew the "react & quench" approach under certain favourable conditions; this in turn has spurred an interest in operando INS studies. [32]

Quasielastic neutron scattering (QENS) concerns low energy motions and the resultant small changes in energy ($\Delta E \sim 0$) i.e., QENS measures the Doppler broadening of a neutron beam scattered from atoms in motion. [33] From quantifying surface hydrogen dissociation temperature [34] to measuring the diffusion constants in microporous materials, [35] QENS yields information about motions occurring over picosecond to nanosecond time scales and Angstrom lengths; [33] providing the most precise means of measuring microporous transport, as indicated by decades of research output. [36-39] Ability to make measurements at higher temperatures renders QENS to be a more suitable technique for operando studies. O'Malley et al., for example, have reported methoxylation within H-ZSM-5 zeolite occurring at room temperature following a combination of in situ QENS and INS measurements, and density functional theory (DFT) calculations. [40] More recently, Martinez et al. documented the first operando QENS investigation of water dynamics in a state-of-the-art ionomer membrane, mounted in a working fuel cell; [41] whilst Silverwood and Garcia Sakai investigated propane diffusion within ZSM-5 and demonstrated, for the first time, a QENS measurement of an adsorbed phase in equilibrium with a flowing gas. [42]

This study presents two recent in situ measurements that could be easily adapted to operando investigations with neutron diffraction and QENS spectroscopy. The diffraction measurement was used to measure

strain within a heterogenous catalyst (SSZ13) as a function of time under dry and 100% humidity conditions; whilst QENS was employed in an attempt to quantify changes in the dynamic behaviour of ligands (i.e., the flexibility of said ligands) within a homogenous catalyst during metal complexation.

Zeolites are widely used as catalysts in the petrochemical industry and beyond, although the interaction between pore walls and sorbates is not well understood. The fact that the pore encompasses the sorbate introduces additional steric effects and restricts diffusion and co-sorption of reactants. Their charged framework provides the possibility of single-site catalysis from metallic cations and they display both Lewis and Brønsted acidity, which is key for their role as solid acid catalysts. The Brønsted acid site has been shown to critically depend on the hydration level of the zeolite due to the formation of hydronium ion-water clusters, [43] and hydrothermal treatment of zeolites post synthesis is often used to dealuminate the framework, either to decrease the number of acid sites or to open meso- and macro-pores to improve diffusion characteristics. [44,45] Reactions in which water is produced as a side product or appears as an impurity in feed streams can therefore modify the catalyst topology and chemical selectivity over time. One such reaction is the selective catalytic reduction of NOx with ammonia that is used in the remediation of vehicle diesel exhaust, which uses a source of ammonia to reduce toxic nitrogen oxides to produce nitrogen and water. Additionally water may be present in the feed from the engine, and the catalyst must remain stable and active over extended time conditions that vary considerable in temperature and feed composition both with time onstream and position in the catalyst monolith. An understanding of the effects of water under reaction conditions is thus of considerable interest, [45] especially as it has

been shown to be beneficial under certain conditions. [46]

Bipyridine and phenanthroline (and related) ligands are widely used within nickel catalysis. [47,48] The reasons for their efficacy in a range of reactions likely stems from their redox non-innocence. [49] The solvents used for these types of reactions are important and are typically very polar and consist of nitriles, alcohols and amides with DMA and DMF appearing regularly. The methanol used in this study has a dielectric constant within the range of the solvents which are most commonly used. However, subtle changes in ligand structure can lead to quite diverse changes in catalyst speciation and catalytic reactivity, [50] and the ligand-catalyst complex is typically formed in situ from a nickel(II) precursor and the ligand. Our aims here were to understand whether we can use QENS to probe the formation of the ligand-catalyst complex in situ, as this is otherwise a very difficult reaction to monitor. If the ligand-catalyst complex does not form during a catalytic reaction, then the reaction will either not proceed, or the catalyst speciation will be different, potentially leading to different reactivity and/or selectivity.

Both studies yielded results that demonstrate the utility of this approach and aim to inspire future operando studies to address other catalytic and chemical systems.

## Experimental
Homogeneous and heterogenous reactions were measured using quasielastic neutron scattering and high-resolution diffraction measurements using the IRIS and Engin-X instruments at the ISIS neutron and muon source in the UK.

## Liquid measurements
QENS measurements of [NiCl$_2$(DME)] and 2,2′-Bipyridine (bpy) reactants in methanol-$d_4$ were made at 320 K along with the pure

solvent. For the complexation reaction, the [NiCl$_2$(DME)] and bpy were mixed immediately before measurement, and data repeatedly acquired for 240 min at 320 K. The IRIS spectrometer was utilised with the pyrolytic graphite (002) analyser which provides an energy transfer window of 1 meV around the elastic peak with a resolution of 0.0175 meV. The total scattering intensity was obtained by integrating between ⁻0.5 and 0.5 meV, with the elastic component integrated over the range ⁻0.0175—0.0175. The inelastic intensity was calculated as the difference between the two, with the EISF derived from these results. All measurements were made in indium-sealed aluminium sample cans with annular geometry to minimise multiple scattering.
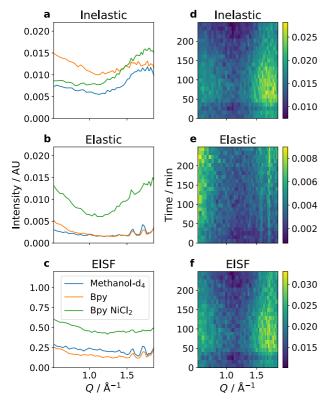


*Figure 1Plots of the integrated scattering intensities a-c showing the Q-dependence of the independent components and d-f the intensity as a function of time for the liquid-phase reaction*

## Solid measurements

Commercial-grade chabazite was kindly supplied by Johnson Matthey. A sample was loaded in a cylindrical plug flow stainless steel reactor of nominal diameter 16 mm with CF flanges sealed with copper gaskets. He gas flow was managed using a custom mass flow controller system supplied by Bronkhorst. Saturated water vapour loading of the gas could be obtained by passing the gas flow through a heated bubbler volume that contained water heated to 42 °C. Trace-heated stainless steel lines transferred the gas to the sample position. Data was collected at the front and rear of the catalyst bed alternately. Only the data collected at the rear of the bed is shown here. To improve the visibility of trends within the data each diffraction peak was fitted to a Gaussian function.

The zeolite was initially treated with water vapour flow with the reactor held at 47 °C. After 133 minutes the water dosing system was bypassed, and dry gas flow was passed through the reactor. At 921 minutes the sample was heated to 80 °C under dry flow.

## Results

## Homogeneous liquid reaction

Plots of the integrated intensities are presented in Figure 1. Plots **a**—**c** show the **Q** dependence of the individual components, with **d**—**f** showing the intensity as a function of time in the reacting system. It is clear from Fig 1a that there is greater inelastic intensity for the solution containing the Bipy NiCl$_2$ complex at higher Q when compared with the other components, indicating greater motion within the dynamic window of the instrument. It is expected that this arises from the mobility of the ligand protons, although solvent dynamics in the solvation sphere cannot be excluded. Either way this indicates improve access to the metal complexation site. Figure 1d shows an increase in the inelastic intensity above 1.5 Å$^{-1}$ from 50 minutes. followed by a drop in intensity that is consistent with the growth and decay of an intermediate in the formation of the metal complex. As this is an *in situ* measurement in a sealed vessel changes cannot be attributed to variation in the total scattering cross section unless components are precipitating and settling out in the bottom portion of the sample can below the beam. This can be

discounted by observing the EISF, which acts as a normalisation to the total scattering. It must therefore be due to a change in the dynamics of the system caused by reaction.

## Heterogenous gas/solid reaction

Figure 2 shows the evolution of selected diffraction peaks from the zeolite catalyst with time as both raw data and fitted Gaussian functions. The first red line corresponds to the switch from water saturated gas flow to dry gas at 133 min. The second red line indicates the onset of heating to 80 °C at 921 min onstream. The peak around 3.53 Å shows the greatest response, with a shift to lower d-spacing with intial water dosing. This continues after the water vapour generator is bypassed up to 400 minutes. This shows slow diffusion of the water within the zeolite pores migrating to the bulk from the surface. After this time the peak position is stable under these conditions. Heating at 921 minutes sees a shift in the peak back to its original position. The peaks at 2.84 and 2.88 Å show less pronounced changes in the initial dosing and continuous dry flow stages, but changes are clear upon the final heating stage. The 2.84 Å peak shows the same trends as the 3.53 Å peak, but the 2.88 Å shows the opposite effect, which demonstrates the anisotropic contraction of the zeolite on water adsorption.
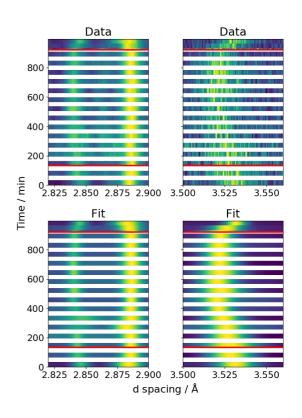


*Figure 2 Diffraction measurement from chabazite catalyst as a function of time. Lines at 133 and 921 min show the termination of water dosing and the onset of heating respectively*

## Discussion

Clear variation in the samples investigated as a function of reaction time confirms the possibility of *operando* neutron scattering in both quasielastic and diffraction regimes under batch and flow conditions. Ligand flexibility in liquid-phase catalysis has dynamic steric affects that affect the direction of reaction and have only been treated in a cursory manner. We have shown that QENS offers a new method to characterise these motions. This work represents the first experiment to show that ligand re-arrangement may be used to follow the reaction in a homogenous catalyst. As with increasingly ligands it becomes more difficult to distinguish electronic and steric effects this provides a way to quantify the dynamic steric inhibition that occurs through ligand displacement around the active metal.

In the solid phase mechanical stress has been shown to affect catalytic activity [51] and that the contraction and expansion of zeolites differs between sorbate gases. [52-54] Changes

in the geometry of zeolitic frameworks will also affect the shape-selectivity of these materials. It is therefore necessary to distinguish the mechanical and chemical effects caused by guest molecules in the pores, especially in the dynamic conditions of co-adsorption and reaction. It is hoped that this work will inspire future measurements facilitated by the penetration of neutrons under more extreme conditions than conventional techniques.

## Declaration

## Acknowledgments

## References

1. A Chakrabarti, ME Ford, D Gregory, R Hu, CJ Keturakis, S Lwin, Y Tang, Z Yang, M Zhu, MA Bañares, IE Wachs (2017) A decade+ of operando spectroscopy studies, Catal. Today 283:27–53

2. EK Gibson, IP Silverwood, PP Wells, SF Parker (2017) In Situ and Operando Measurement of Catalysts at Synchrotron X-ray and Neutron Sources in Modern developments in catalysis, World Scientific. Eds. G Hutchings, M Davidson, CRA Catlow, C Hardacre, N Turner, P Collier

3. MA Bañares, MO Guerrero-Pérez, JLG Fierro, GG Cortez, Raman spectroscopy during catalytic operations with on-line activity measurement (operando spectroscopy): A method for understanding the active centres of cations supported on porous materials (2002) J. Mater. Chem. 12:3337–3342

4. D Goonetilleke, N Sharma (2019) In situ neutron powder diffraction studies, Phys. Sci. Rev. 6:20180155

5. PA Wright, JM Thomas, AK Cheetham, AK Nowak (1985) Localizing active sites in zeolitic catalysts: Neutron powder profile analysis and computer simulation of deuteropyridine bound to gallozeolite-L, Nature 318:611–614

6. R Goyal, AN Fitch, H Jobic (2000) Powder Neutron and X-ray Diffraction Studies of Benzene Adsorbed in Zeolite ZSM-5, J. Phys. Chem. B 104:2878–2884

7. M Falkowska, , S Chansai, HG Manyar, LF Gladden, DT Bowron, TGA Youngs C Hardacre (2016) Determination of toluene hydrogenation kinetics with neutron diffraction, Phys. Chem. Chem. Phys. 18:17237–17243

8. F Fauth, E Suard, J-B Leriche, C Masquelier L Croguennec (2015) Spinel materials for Li-ion batteries: New insights obtained by operando neutron and synchrotron X-ray diffraction, Acta Cryst. B 71:688–701

9. FG Kinyanjui, ST Norberg, I Ahmed, SG Eriksson, S Hull (2012) In-situ conductivity and hydration studies of proton conductors using neutron powder diffraction, Solid State Ionics 225:312–316

10. T Kandemir, D Wallacher T Hansen, K-D Liss, R Naumann d'Alnoncourt, R Schlögl M Behrens (2012) In situ neutron diffraction under high pressure - Providing an insight into working catalysts, Nucl. Instrum. Methods A 673:51–55

11. T Kandemir, F Girgsdies, TC Hansen, K-D Liss, I Kasatkin, EL Kunkes, G Wowsnick, N Jacobsen, R Schlögl, M Behrens (2013) In Situ study of catalytic processes: Neutron diffraction of a methanol synthesis catalyst at industrially relevant pressure, Angew. Chem. Int. Ed. 52:5166–5170

12. M Hirscher, VA Yartys, A Volodymyr, M Baricco (2020) Materials for hydrogen-based energy storage - past, recent progress and future outlook, J. Alloys Compd. 827:153548

13. T. Kandemir, ME Schuster, A Senyshyn, M Behrens, R Schlögl (2013) The Haber-Bosch process revisited: On the real structure and stability of 'ammonia iron' under working conditions, Angew. Chem. Int. Ed. 52:12723–12726

14. JW Makepeace, TJ Wood, HMA Hunter, MO Jones, WIF David (2015) Ammonia decomposition catalysis using non-stoichiometric lithium imide. Chem. Sci. 6:3805–3815

15. JW Makepeace, TJ Wood, PL Marks, RI Smith, CA Murray, WIF David (2018) Bulk phase behavior of lithium imide-metal nitride ammonia decomposition catalysts, Phys. Chem. Chem. Phys 20:22689–22697

16. TJ Wood, JW Makepeace, WIF David (2018) Neutron diffraction and gravimetric study of the manganese nitriding reaction under ammonia decomposition conditions, Phys. Chem. Chem. Phys. 20:8547–8553

17. PCH Mitchell, SF Parker, AJ Ramirez-Cuesta, J Tomkinson (2005) Vibrational Spectroscopy with Neutrons, with applications in Chemistry, Biology, Materials Science and Catalysis. World Scientific

18. VF Sears (1992) Neutron scattering lengths and cross sections, Neutron News 3:26–37

19. S Bösing, G Prescher, K Seibold, DK Ross, SF Parker (1999) Inelastic neutron scattering investigations of the products of thermally and catalytically driven catalyst coking, Appl. Catal. A 187:233–243

20. P Albers, H Angert, G Prescher, K Seibold, SF Parker (1999) Catalyst poisoning by methyl groups, Chem. Commun. 1999:1619–1620

21. IP Silverwood, NG Hamilton, JZ Staniforth, CJ Laycock, SF Parker, RM Ormerod, D Lennon (2010) Persistent species formed during the carbon dioxide reforming of methane over a nickel-alumina catalyst, Catal. Today 155:319–325

22. IP Silverwood, NG Hamilton, CJ Laycock, JZ Staniforth, RM Ormerod, CD Frost, SF Parker, D Lennon (2010) Quantification of surface species present on a nickel/alumina methane reforming catalyst, Phys. Chem. Chem. Phys. 12:3102–3107

23. PW Albers, J Pietsch, J Krauter, SF Parker (2003) Investigations of activated carbon catalyst supports from different natural sources, Phys. Chem. Chem. Phys. 5:1941–1949

24. S Chinta, TV Choudhary, LL Daemen, J Eckert, DW Goodman (2002) Characterization of C2 (CxHy) intermediates from adsorption and decomposition of methane on supported metal catalysts by in situ INS vibrational spectroscopy, Angew. Chem. Int. Ed. 41:144–146

25. D Lennon, J McNamara, JR Phillips, RM Ibberson, SF Parker (2000) An inelastic neutron scattering spectroscopic investigation of the adsorption of ethene and propene on carbon, Phys. Chem. Chem. Phys. 2, 4447–4451

26. AR McInroy, DT Lundie, JM Winfield, CC Dudman, P Jones, SF Parker, JW Taylor, D Lennon (2005) An infrared and inelastic neutron scattering spectroscopic investigation on the interaction of η-alumina and methanol, Phys. Chem. Chem. Phys. 7:3093–3101

27. A Griffin, H Jobic (1981) Theory of the effective Debye–Waller factor in neutron scattering from high frequency molecular modes, J. Chem. Phys. 75:5940–5943

28. AJ O'Malley, SF Parker, CRA Catlow (2017) Neutron spectroscopy as a tool in catalytic science, Chem. Commun. 53:12164–12176

29. SF Parker, P Collier (2016) Applications of neutron scattering in catalysis. Johnson Matthey Technol. Rev. 60:132–144

30. IP Silverwood, NG Hamilton, A McFarlane, RM Ormerod, T Guidi, J Bones, MP Dudman, CM Goodway, M Kibble, SF Parker, D Lennon (2011) Experimental arrangements suitable for the acquisition of inelastic neutron scattering spectra of heterogeneous catalysts, Rev. Sci. Instrum. 82:034101

31. SF Parker (2011) The role of hydroxyl groups in low temperature carbon monoxide oxidation. Chem. Commun. 47, 1988–1990

32. SF Parker, AJ Ramirez-Cuesta, PW Albers, D Lennon (2014) The use of direct geometry spectrometers in molecular spectroscopy, J. Phys. Conf. Ser. 554:012004

33. M Bée (1988) Quasielastic Neutron Scattering, Principles and Applications in Solid State Chemistry, Biology and Materials, Taylor and Francis

34. SF Parker CD Frost M Telling P Albers M Lopez K Seitz (2006) Characterisation of the adsorption sites of hydrogen on Pt/C fuel cell catalysts. Catal. Today 114:418–421

35. H Jobic, DN Theodorou (2007) Quasi-elastic neutron scattering and molecular dynamics simulation as complementary techniques for studying diffusion in zeolites, Micropor. Mesopor. Mater. 102:21–50

36. CJ Wright, C Riekel, (1978) The uniaxial rotation of ethylene adsorbed by sodium 13X zeolite. Mol. Phys. 36:695–704

37. R Stockmeyer (1997) Ethanol in chabazite at temperatures between 300 and 440 K studied by neutron time-of-flight spectroscopy, Phys. B Condens. Matter 234–236:917–918

38. VK Sharma, MN Rao, S Gautam, AK Tripathi, VS Kamble, SL Chaplot R Mukhopadhyay (2008) Rotational dynamics of propylene inside Na-Y zeolite cages, Pramana 71:1165–1169

39. AJ O'Malley, V García Sakai, IP Silverwood, N Dimitratos, SF Parker, CRA Catlow (2016) Methanol diffusion in zeolite HY: A combined quasielastic neutron scattering and molecular dynamics simulation study, Phys. Chem. Chem. Phys. 18:17294–17302

40. AJ O'Malley, SF Parker, A Chutia, M Farrow, IP Silverwood, V García Sakai, CRA Catlow (2016) Room temperature methoxylation in zeolites: Insight into a key step of the methanol-to-hydrocarbons process, Chem. Commun. 52:2897–2900

41. N Martinez, A Morin, Q Berrod, B Frick, J Ollivier, L Porcar, G Gebel, S. Lyonnard (2018) Multiscale Water Dynamics in a Fuel Cell by Operando Quasi Elastic Neutron Scattering, J. Phys. Chem. C 122:1103–1108

42. IP Silverwood, V García Sakai (2018) Propane diffusion in ZSM-5 pores measured by quasielastic neutron scattering under macroscopic flow, Chem. Eng. Sci. 186:116–121

43. M. Wang, NR Jaegers, M-S Lee, C Wan, JZ Hu, H Shi, D Mei, SD Burton, DM. Camaioni, OY. Gutiérrez, V-A Glezakou, R Rousseau, Y Wang, JA Lercher (2019) Genesis and Stability of Hydronium Ions in Zeolite Channels, J. Am. Chem. Soc. 141:3444–3455

44. M. Maache, A. Janin, J.C. Lavalley, E. Benazzi (1995) FT infrared study of Brønsted acidity of H-mordenites: Heterogeneity and effect of dealumination, Zeolites, 15:507–516,

45. L Ma, Y Cheng, G Cavataio, RW. McCabe, L Fu, J Li (2013) Characterization of commercial Cu-SSZ-13 and Cu-SAPO-34 catalysts with hydrothermal treatment for NH3-SCR of NOx in diesel exhaust, Chem. Eng. J. 225:323–330,

46. H-Y Chen, WMH Sachtler (1998) Activity and durability of Fe/ZSM-5 catalysts for lean burn NOx reduction in the presence of water vapor, Catal. Today 42:73–83

47. J Twilton, C Le, P Zhang, MH Shaw, RW Evans DWC MacMillan (2017) The merger of transition metal and photocatalysis, Nature Rev. Chem. 2017, 1:0052

48. DJ Weix (2015) Methods and Mechanisms for Cross-Electrophile Coupling of Csp2 Halides with Alkyl Electrophiles, Acc. Chem. Res. 2015 48:1767–1775

49. JT Ciszewski, DY Mikhaylov, KV Holin, MK Kadirov, YH Budnikova, O Sinyashin, DA Vicic (2011) Redox Trends in Terpyridine Nickel Complexes, Inorg. Chem. 50:8630-8635

50. 56 M Mohadjer Beromi, GW Brudvig, N Hazari, HMC Lant, BQ Mercado, (2019) Synthesis and Reactivity of Paramagnetic Nickel Polypyridyl Complexes Relevant to C(sp2)–C(sp3)Coupling Reactions, Angew. Chem. Int. Ed. 58:6094.

51. AR Passos, A Rochet, LM Manente, AF Suzana, R Harder, W Cha, F Meneau (2020) Three-dimensional strain dynamics govern the hysteresis in heterogeneous catalysis, Nature Commun. 11:4733

52. B Ilić, SG Wettstein (2017) A review of adsorbate and temperature-induced zeolite framework. Miropor. Mesopor. Mater. 239:221-234

53. SG Sorenson, JR Smyth, RD. Noble, JL Falconer (2009) Correlation of Crystal Lattice Expansion and Membrane Properties for MFI Zeolites, Ind. Eng. Chem. Res. 48:10021-10024

54. GY Gor, P Huber, N Bernstein (2017) Adsorption-induced deformation of nanoporous materials, Appl. Phys. Rev.4:011303

55. David Nelson & Ian Silverwood (2018) Towards Active Site Orientation Kinetics in Solution with Quasielastic Neutron Scattering. STFC ISIS Neutron and Muon Source,
https://doi.org/10.5286/ISIS.E.97999717

56. Andrew York. (2020) An attempt to measure sorption through strain induced deformation. STFC ISIS Neutron and Muon Source,
https://doi.org/10.5286/ISIS.E.RB1920712

# Supporting information for:
# *Operando* Neutron Scattering – Following Reactions in Real Time Using Neutrons

k

**SYNTHESIS**

**General.** Nickel dichloride hexahydrate was obtained from Preston Chemicals and used to prepare [NiCl₂(DME)] according to a literature method[1]. 2,2'-Bipyridine (bpy) was obtained from Fluorochem and methanol-$d_4$ was obtained from Sigma-Aldrich. Methanol was obtained from Fisher Scientific and dried on magnesium/iodine and distilled prior to use.

**[NiCl₂(bpy)].** Dimethoxyethane nickel dichloride (657 mg, 3 mmol), 2,2'-bipyridine (468 mg, 3 mmol) and a magnetic stirrer bar were loaded into a microwave vial followed by dry methanol (3 mL). The vial was sealed with a septum-fitted cap and the reaction was stirred at room temperature overnight. The reaction mixture was then transferred to a round bottom flask before the addition of diethyl ether (10 mL). The resulting precipitate was isolated by vacuuum filtration. The precipitate was then washed with ethanol (10 mL) and diethyl ether (2 x 10 mL). The product is a dry free flowing green powder which was weighed and transferred to a labelled vial (85% yield). **$^1$H NMR** (D₃OD, 400 MHz): $\delta_H$ = 157.09 ppm (br s), 58.67 (br s), 43.20 (br s), 14.81 (br s).

**ANALYSIS**

**Static Samples.** Saturated solutions were prepared of each analyte and loaded into vanadium cans. In each case, 0.25 mL of solution was used.

Bpy:               0.246 g in 1 mL D₃OD                 (30% *w/w*)
[NiCl₂(bpy)]:      0.108 g in 1 mL D₃OD                 (12% *w/w*)

***In Situ* Reaction Samples.** Solutions of each component were mixed in a vanadium can prior to analysis. [NiCl₂(DME)] was found to be soluble to 20% *w/w* and bpy to 30% *w/w*. The product [NiCl₂(bpy)] was found to be soluble to *ca.* 12-14% *w/w* so the experiment was designed to give a conversion of product in solution at 12.8% by weight in D₃OD.

(DME)NiCl₂:      42 mg in 0.5 mL D₃OD           0.125 mL of solution used for analysis
BIPY:             30 mg in 0.5 mL D₃OD           0.125 mL of solution used for analysis

1. Ward, L. G. L., & Pipal, J. R. (2007). Anhydrous Nickel(II) Halides and their Tetrakis(ethanol) and 1,2-Dimethoxyethane Complexes. Inorganic Syntheses, 154–164. doi:10.1002/9780470132449.ch30